Available online at www.sciencedirect.com
ScienceDirect
Ceramics International 37 (2011) 1063–1072
CERAMICS INTERNATIONAL
www.elsevier.com/locate/ceramint

In situ growth of silicon carbide nanowires from anthracite surfaces

He Huang [a], John T. Fox [a], Fred S. Cannon [a], Sridhar Komarneni [b,*]

[a] Department of Civil and Environmental Engineering, The Pennsylvania State University, University Park, PA 16802, USA
[b] Materials Research Institute and Department of Crop and Soil Sciences, The Pennsylvania State University, University Park, PA 16802, USA

Received 2 August 2010; received in revised form 16 October 2010; accepted 15 November 2010
Available online 3 December 2010

Abstract

Silicon carbide nanowires (SCNWs) were grown from anthracite fine surfaces through a simple one-step carbothermal process with silicon powder as the Si precursor. This straightforward and fast formation of SCNWs made it possible to maintain the binding of briquetted waste anthracite fines at very high temperatures as an alternative fuel in foundry cupola furnaces. This SCNW mechanism could thus provide the crucial hot crushing strength in the cupola heat zone and melt zone. Progressive thermal tests exhibited that the formation of the SCNWs started from 1100° C, and was favored at 1400° C. No extra metal catalyst was needed for the growth of the SCNWs. Characterizations were performed by XRD, SEM, EDS, TEM, and SAED. The SCNWs were 30–60 nm in diameter and were typically grown by stacking the (1 1 1) lattice plane of 3C-SiC along the [1 1 1] direction. Many non-epitaxial branches of the nanowires were also formed through this one-step process as observed by TEM. The results suggest that the SCNWs were most likely grown through the vapor–solid mechanism.

Keywords: Ceramic reinforcement; Sustainable engineering; Chemical vapor deposition

1. Introduction

Silicon carbide is a ceramic material with extraordinary mechanical properties, and it is frequently employed to reinforce other ceramic materials [1,2]. Silicon carbide nanowires (SCNWs) could be grown from many different substrates [3–5], including carbon-based materials [6,7]. SCNWs have received much attention partially due to their electronic properties and their high mechanical strength even at extremely high temperatures [8–10]. Rapid formation of silicon carbide nanowires in situ offers an important mechanism when devising an alternative to coke in iron foundry cupolas. Briquetted fuels, such as briquetted anthracite fines could be a much cheaper and cleaner replacement for the depleting foundry coke, which was produced by pyrolyzing special coking bituminous coal through an energy intensive process. However, anthracite bricks bound by typical binders could not maintain their structural integrity to provide the crucial hot crushing strength in the cupola preheat and melting zone. By combining the silicon source used in iron melting process with the briquetted anthracite fines, one hypothesis is that SCNWs will form under the carbothermal condition in the cupola preheat zone to provide mechanical strength for the briquetted anthracite bricks.

Although various precursors and processes have been employed [11–15] to produce SCNWs, most protocols rely on chemical vapor deposition via either vapor–liquid–solid (VLS) [16,17] or vapor–solid (VS) mechanisms [18]. Usually these processes have required a continuous supply of silicon and carbon precursors to provide raw materials for the growth of the nanowires. Yet further, metallic catalysts have generally been invoked for forming the liquid phase in VLS growths that has led to the growth of the nanowires. In contrast, metallic catalysts are not necessary for VS growths.

In contrast to the complex protocols documented by others, in this study a simplified process has been devised for growing SCNWs on the surface of anthracite fines. Silicon powders were combined with anthracite fines and exposed to thermal conditions that simulated the cupola preheat zone. Yet further, the SCNWs generated herein were then tested so as to discern their mechanical strength for binding the anthracite fines together after exposure to extremely high temperatures. For

* Corresponding author at: 205 Materials Research Laboratory, The Pennsylvania State University, University Park, PA 16802, USA.
Tel.: +1 814 865 1542; fax: +1 814 865 2326.
E-mail address: Komarneni@psu.edu (S. Komarneni).

0272-8842/$36.00
doi:10.1016/j.ceramint.2010.11.022

full-scale foundry fuel applications there are several fundamental scientific questions that were associated with the environment that the SCNWs were proposed to be applied in. First, carbothermal conditions exist in the cupola preheat zone (1000–1400 °C) which is above the cupola melting zone where all oxygen is consumed in burning carbon [19]. The first question was whether the SCNWs could grow quickly within this 1000–1400 °C temperature range. Secondly, the anthracite fines contain considerable traces of metals, and the question was whether these helped catalyze the growth of the SCNWs. The third question was whether the in situ solid anthracite and silicon could rapidly undergo mechanisms of volatilization and re-condensation to such an extent that no supplemental gas-phase source of carbon or silicon would be needed.

In this study, analytical techniques such as scanning electron microscopy (SEM), energy dispersive X-ray spectroscopy (EDS), transmission electron microscopy (TEM), and X-ray diffraction (XRD) were employed to monitor the morphology and crystallography changes in the silicon and anthracite system. In order to simulate cupola conditions, the authors focused on how the pyrolysis temperature and silicon content affected the growth of SCNWs.

2. Experimental procedure

2.1. Raw materials

The anthracite fines used in this study were obtained from Jeddo Coal Company (Hazelton, PA). The elemental analysis of this coal source has been listed in Table 1. As tested by sieve analysis, most of these anthracite grains (about 97%) were within the range of U.S. mesh #10 × 80 (2000–179 μm). This grain size has been identified as ''anthracite fines'' throughout the text herein.

The silicon metal was purchased from Alfa Aesar (Ward Hill, MA) as 98.4% silicon lumps. The lumps were crushed into silicon powders by a SPEX 8000 mixer/mill from A.O. Smith Corp. (Milwaukee, WI) with 8 steel balls for 10 min, and then screened to less than U.S. mesh #100 (150 μm) sieve. The typical grain size of this silicon powder was 10–20 μm as observed by SEM.

2.2. Preparation of anthracite pellets

Anthracite fines were dried at 105 °C overnight to remove the moisture content. Then 100 g of anthracite fines were mixed with 10 g of silicon powder (i.e. 9% Si) unless otherwise stated. In some cases, 2 or 5 g of silicon was used. Also collagen binder (1 g by dry weight) was dissolved in 12 g of water at 70 °C to form a gelatin sol. The anthracite and silicon mixture were added into this sol with constant hand mixing by a glass stick. The final mixture was packed into a cylindrical mold (2.9 cm diameter × 4.8 cm long) with about 280 kPa pressure applied on both ends. Finally, the pellet was extruded from the mold and cured under ambient conditions for 24 h. During this ambient temperature curing, the pellets lost 90% of their water. At least three anthracite pellets were produced for each recipe and protocol, so as to achieve statistical replication.

2.3. The pyrolysis process

The pyrolysis of the anthracite pellets was conducted in a horizontal alumina tube furnace that was 40 cm long and 5 cm in diameter. A slow nitrogen gas flow (∼2 standard cubic centimeters per minute) was used to prevent the anthracite from burning. In some cases, no nitrogen flow was applied, and effectively a starved air condition was established within the tube furnace, for which the oxygen within the chamber burned 0.08 g carbon (<0.3% of the pellet mass). Strength and SEM results were no different when using N_2 flow or starved air. A three-step pyrolysis procedure was employed. First the furnace was ramped up to the prescribed temperature at 3 °C/min. Then this prescribed temperature was maintained for 2 h. Finally the furnace was cooled down to room temperature at 3 °C/min again. In order to protect the furnace and the tube, heating or cooling rates that are faster than 3 °C/min were not employed. The pyrolyzed anthracite pellets were then removed from the tube-furnace for further tests. Unless otherwise identified, the prescribed maximum temperature was 1400 °C, which is close to the temperature that the anthracite bricks would encounter in the preheating zone of a cupola furnace. As identified below, other prescribed temperatures of 1000–1300 °C were also tested so as to investigate the crystal structure change in the system as the temperature increased.

2.4. SEM, EDS, and TEM

SEM and EDS were performed on an FEI Quanta 200 Environmental SEM. The instrument was operated under low-vacuum conditions (10–103 Pa) using a Gaseous SE detector. The high voltage was set at 20 kV and the spot size of the electron beam was set at 4 nm. The EDS spectrums were collected from 0 to 10 keV within 60-s.

A transmission electron microscope (TEM, Model 2010, JEOL, Tokyo, Japan) was used for electron diffraction, and to determine the morphology and particle size.

Table 1
Elemental analysis of anthracite fines used in this study.

Proximate analysis %				Ultimate analysis % (dry, ash free)				
Moisture	Volatile matter (dry)	Fixed carbon (dry)	Ash (dry)	C	H	N	S	O
3.0	4.99	82.3	12.8	94.3	2.25	0.89	0.38	2.59

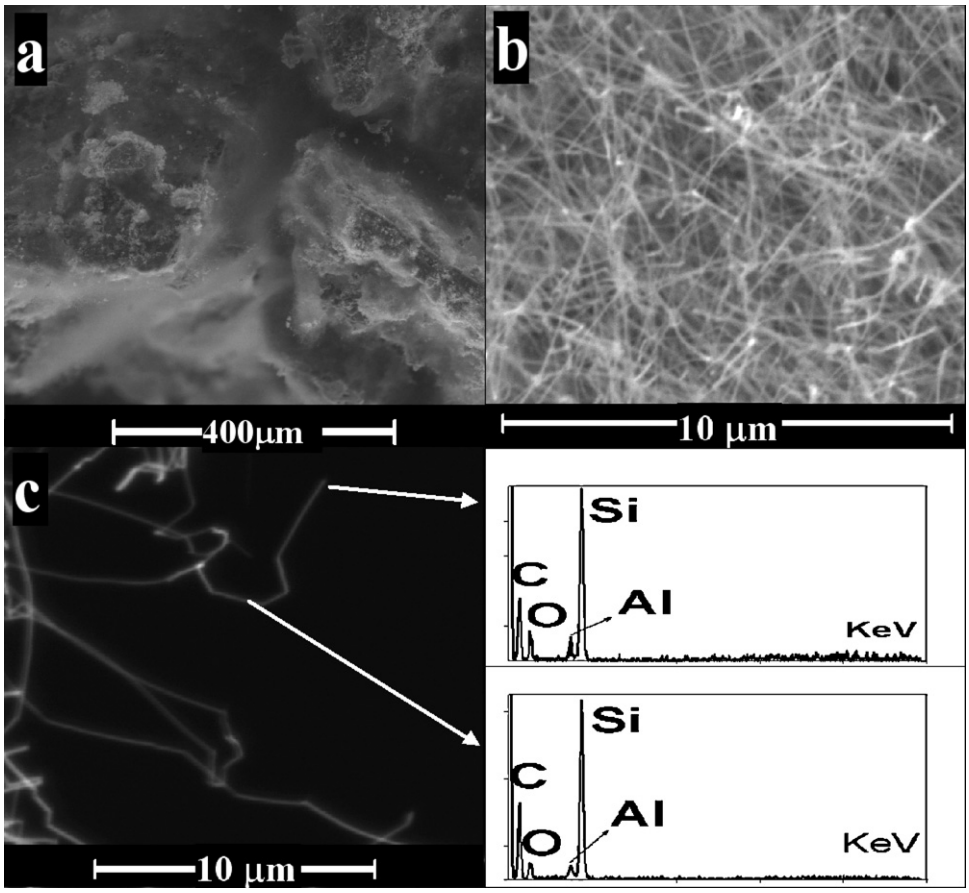

Fig. 1. SEM images of silicon carbide nanowires grown from anthracite fines (with 9% silicon and 1% collagen) at 1400 °C, and EDS spectrums from different locations on a nanowire.

2.5. Ambient-temperature XRD and real-time high-temperature XRD

Ambient temperature XRD patterns were obtained via a PANalytical X'Pert Pro MPD diffractometer. The diffraction pattern within 2θ of 5–70° was collected. For these analyses, the pellets were crushed into powders by the ball mill and placed into a special aluminum powder sample holder. So the powder XRD pattern was a bulk measurement and represented the average situation in the pyrolyzed pellets.

Real-time high-temperature XRD tests were also performed on the PANalytical X'Pert Pro MPD diffractometer. The anthracite pellets were pulverized before the pyrolysis. Next, the powders that contained both silicon and anthracite without collagen binder were placed on an alumina strip. A vacuum condition was provided around the alumina and the strip was heated from room temperature to 1400 °C at 100 °C per minute. Once the temperature reached 1400 °C, the diffractometer started to collect diffraction signals from 10° to 70° repeatedly. Each scan from 10° to 70° took about 7 min, so the real time change of the XRD pattern at 1400 °C could be observed in this way.

2.6. Unconfined compressive strength

The unconfined compressive strength after pyrolysis was used to simulate key features of the hot crushing strength within a cupola. The unconfined compressive strength of the pyrolyzed anthracite pellets were determined by a Simpson-Gerosa electronic universal sand strength machine (model 42104). A horizontally moving arm applied pressure on an unconfined pellet until failure. The final unconfined compressive strength was calculated based on the cross sectional area of the original pellet sample.

3. Results and discussion

3.1. SEM and TEM of the SCNWs formed at 1400 °C

Pellets that contained 9% silicon, 1% collagen, and 90% anthracite fines were pyrolyzed at 1400 °C. After the thermal treatment, the surface of the anthracite pellets turned from black to light green. This change in color indicated that the surface of the anthracite fines had been covered by the pyrolysis products. The pellets had a post-pyrolysis unconfined compressive strength of 690 kPa.

The SEM images of these treated anthracite fines in Fig. 1 show that intensive SCNWs were formed from the surface of the anthracite fines, and they almost covered the anthracite fines entirely. The high resolution SEM images in Fig. 1b show that the SCNWs grew into a massive network that extended from the anthracite grains' surfaces. In order to discern whether metal catalysts played a role in nanowires formation, EDS was

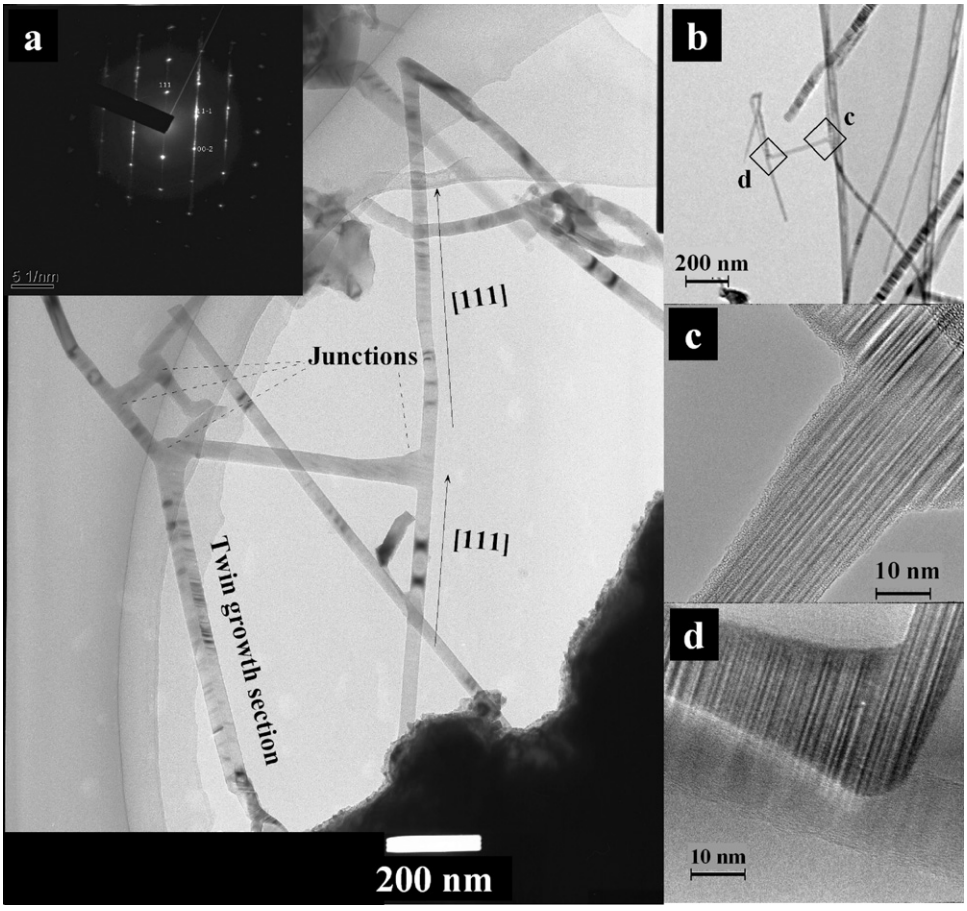

Fig. 2. TEM image of the SCNWs grown from anthracite fines (with 9% silicon and 1% collagen) at 1400 °C. The up corner insert in (a) is the selected area electron diffraction pattern of the SCNWs.

conducted extensively at numerous locations to compare the tips and length of the nanowires. Fig. 1c depicts an example of such a comparison. The EDS responses were about the same in the tips and length of the nanowires, exhibiting that carbon and silicon were the major elements with trace amounts of oxygen and aluminum.

The TEM images of the nanowires (Fig. 2a) exhibited nanowire diameters from 30 to 60 nm. One important feature of the SCNWs growth found in this study is that many of the SCNWs joined to one another at junctions. Some SCNWs joined almost perpendicular into other SCNWs. It appeared that at many such junctions, one of the wires would often stop growing as it teed into another. From the structural view point, these junctions were perceived as desirable in the binding application as they provided extra strength for the anthracite bricks. The trace of stacking of the 3C-SiC (1 1 1) lattice planes along the [1 1 1] direction could be identified from some portions of the SCNWs with high density stack faults in Fig. 2a. Also in the upper-left corner of Fig. 2a, the [−1,1,0] zone diffraction pattern from a nanowire suggested that stack faults were present on the (1 1 1) planes. This [1 1 1] growth is typical for SCNWs [16,20–22]. In the lower left corner of Fig. 2a, twin growth of two SCNWs was also observed, which normally shows a 70.5° between the growth direction and the (1 1 1) plane [16,23,24].

Further investigations of these branching points by HRTEM (Fig. 2b–d) revealed that these branchings were different from the typical epitaxial growth of branched nanowires. Specifically at the branching point, it seemed that the (1 1 1) lattice planes of the backbone nanowires extruded out and formed the branching nanowires. The stacking faults in the branching nanowires indicated that the growth direction of this particular branching nanowire was normal to the nanowires axial. However, this type of growth appeared to not continue sustainably. For example as seen in the TEM image of Fig. 2d, a nanowire that was growing normal to the nanowire axial appeared to bend back to the typical growth direction which is parallel to the axial.

3.2. Post-pyrolysis and real-time high temperature XRD

XRD patterns appear in Fig. 3 for raw anthracite, pyrolyzed anthracite, raw anthracite fines with 9% silicon powder and 1% collagen, and the blend of anthracite, 9% silicon powder and 1% collagen after the 1400 °C pyrolysis. As shown, some crystallized silicate species appeared even in the raw anthracite. These silicates were mainly quartz, muscovite, and kaolinite. After the pyrolysis at 1400 °C, the crystal structure of that anthracite's silicates changed dramatically. The distinctive quartz peaks of the raw materials mostly disappeared in the pyrolyzed anthracite. The kaolinite and muscovite that had

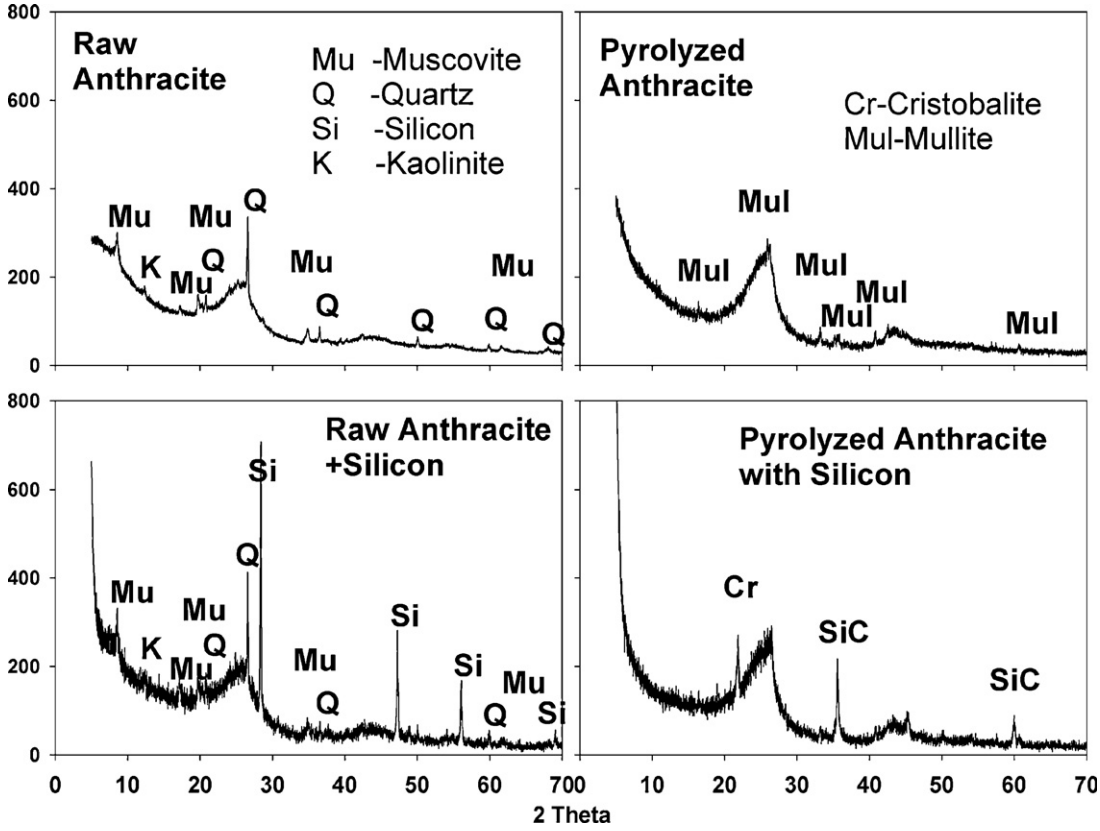

Fig. 3. XRD patterns of raw anthracite fines, and anthracite fines with 9% silicon powders and 1% collagen before and after thermal treatment at 1400 °C.

been found in the raw materials transformed into mullite by the thermal treatment [25]. Meanwhile the carbon structure in the anthracite became more organized after the pyrolysis, as detected in the XRD.

When silicon powders were pyrolyzed together with the anthracite fines at 1400 °C for 2 h, the elemental silicon was depleted. Meanwhile, diffraction peaks from 3C-SiC were found in the post-pyrolysis XRD patterns. Also, the 1400 °C pyrolysis yielded cristobalite (SiO_2) which had not been present in the raw materials but formed when kaolinite transformed to mullite with the excess silica.

Real-time high temperature XRD analysis was also conducted as a mixture of 10% silicon and 90% anthracite fines was pyrolyzed up to 1400 °C. As shown by Fig. 4 XRD responses, 3C-SiC formed within 7 min of this sample reaching 1400 °C. By the time the temperature reached 1400 °C, the elemental silicon had already disappeared from the XRD pattern. Diffraction peaks from the (1 1 1) lattice plane of 3C-SiC appeared in the second scan at 1400 °C. The intensity of this response did not significantly increase with yet further time than 14 min. Indeed, even after 2 h at 1400 °C, this SiC intensity had not increased.

3.3. The effect of pyrolysis temperature on the development of the SCNWs

The effect of pyrolysis temperature on the development of the SCNWs was also appraised. These tests employed pellets made from anthracite fines with 9% silicon powder and 1% collagen binder. For these tests, the pyrolysis chamber ramped temperatures up to the maximum shown (1000–1400 °C), and held at that temperature for 2 h; then the temperature was ramped to ambient. The XRD patterns showed no peak for SiC at 1000 °C. Then by 1100 °C, slight peaks for SiC appeared, and these peaks became somewhat higher at 1200 °C, and yet higher at 1400 °C (Fig. 5). The Si peaks that appeared at 25 °C, 1000 °C, and 1100 °C had become far less intense at 1200 °C, then virtually disappeared at 1400 °C. The quartz peaks that appeared up to 1200 °C were not present at 1400 °C, whereas cristobalite appeared at 1400 °C, but not at lower temperatures.

With regard to physical strength, at 1000 °C, the anthracite pellets lost all their structural integrity and became piles of fines, since the collagen adhering bonds had become broken by 1000 °C, but no SiC nanowires had yet formed. Indeed, at 1000 °C, most of the silicon powders were still in the elemental cubic crystal structure per Fig. 5 and Fig. 6. However, trace amounts of carbon and oxygen were detected by EDS (Fig. 6d) on the surface of the silicon powders.

When the maximum thermal treatment temperature was increased to 1100 °C, the anthracite pellet could hold its shape after the pyrolysis, and offered an unconfined compressive strength of 70 kPa. After 1200 °C pyrolysis the unconfined compressive strength increased to 400 kPa, and after 1400 °C pyrolysis this strength increased yet further to 690 kPa.

The SEM images offered results that were consistent with the XRD and unconfined compressive strength tests. SEM

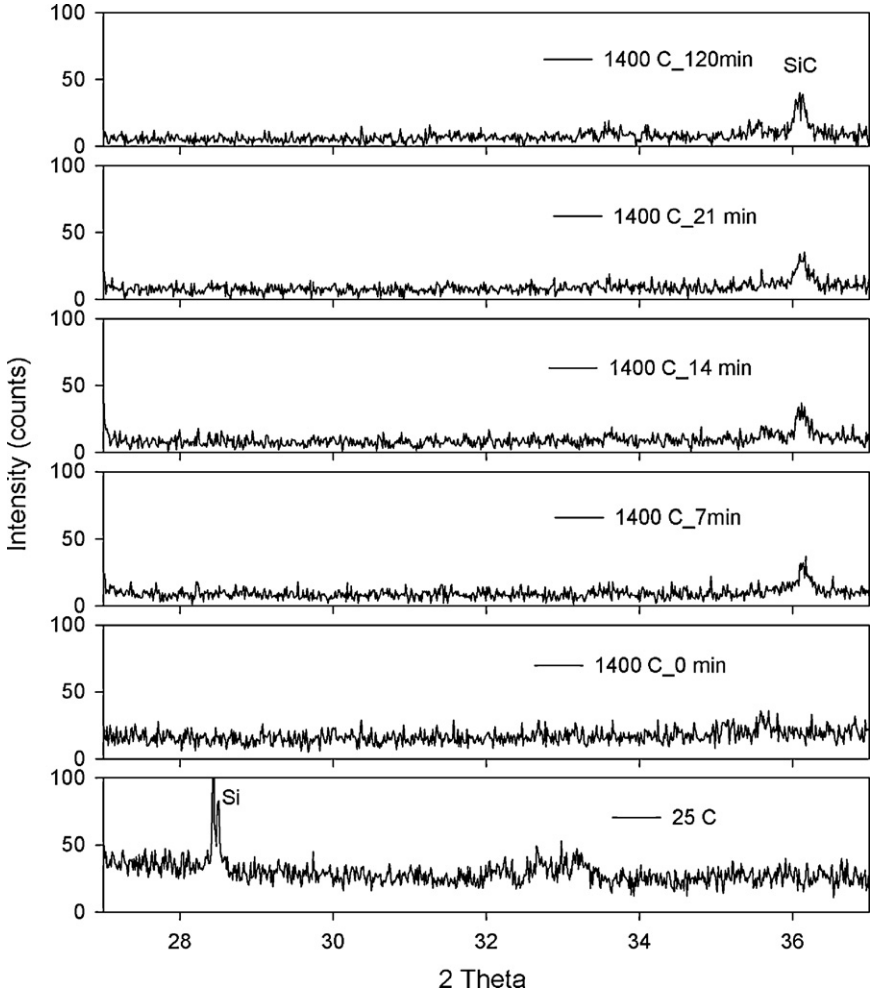

Fig. 4. Real-time change of the XRD pattern at 1400 °C within mixed anthracite and silicon powders (9% silicon and 91% anthracite).

revealed no SCNWs at 1000 °C, some SCNW formation after 1100 °C, and more SCNW formation at 1200 °C (Fig. 6). However the SCNW formation at 1200 °C was considerably less than at 1400 °C, and this was reflected in the lower unconfined compressive strength at lower temperatures.

3.4. The effect of silicon content on the growth of SCNWs

In order to determine the effect of less silicon in these pellet mixtures, pellets with 4.72% and 1.94% silicon were made by using the anthracite fines and pyrolyzed at 1400 °C, following the same pyrolysis procedure as above. The SEM images of these pyrolyzed anthracite pellets are shown in Fig. 7. As compared to Fig. 1, it is clear that the proportion of silicon powder decisively impacted the growth of the nanowires. With 4.72% silicon (Fig. 7a), the anthracite fines were not covered by SCNWs as heavily as they had been when the pellets included 9% silicon. Nonetheless, the nanowires grew very well (Fig. 7b), and their morphology was similar to those that had developed when 9% silicon was included. When the silicon content decreased to 1.74%, the SCNWs did not grow very well with such low silicon content. As shown in Fig. 7d, only a very thin layer of milky material became attached to the surface of the anthracite fine. It was hard to find a single distinct nanowire from this pyrolyzed sample.

3.5. Discussion on the growth mechanism

It is known that SCNWs can be grown through either a VLS or VS mechanism. Metal catalysts are usually important for the formation of the interim liquid phase in VLS growth, but metal catalysts need not be included for the VS growth. Although metallic catalysts were not added into the system, plenty of natural metals (such as Al and Fe) were present in the anthracite that was tested in this study. Others have used iron as the catalyst for SCNW growth [26–28], and aluminum has also been reported to catalyze the growth of SCNWs [29]. However, there was no direct evidence herein to verify that the SCNWs were grown via a VLS route that involved metal catalysts. Indeed, after exhaustively searching via SEM, TEM, and EDS analysis, no clear image of metal spheres at the nanowire tips was observed. EDS spectrums at the nanowires tips showed similar compositions as those in the middles of the nanowires. Also the formation of massive nanowires on the anthracite surface requires tremendous amount of metal

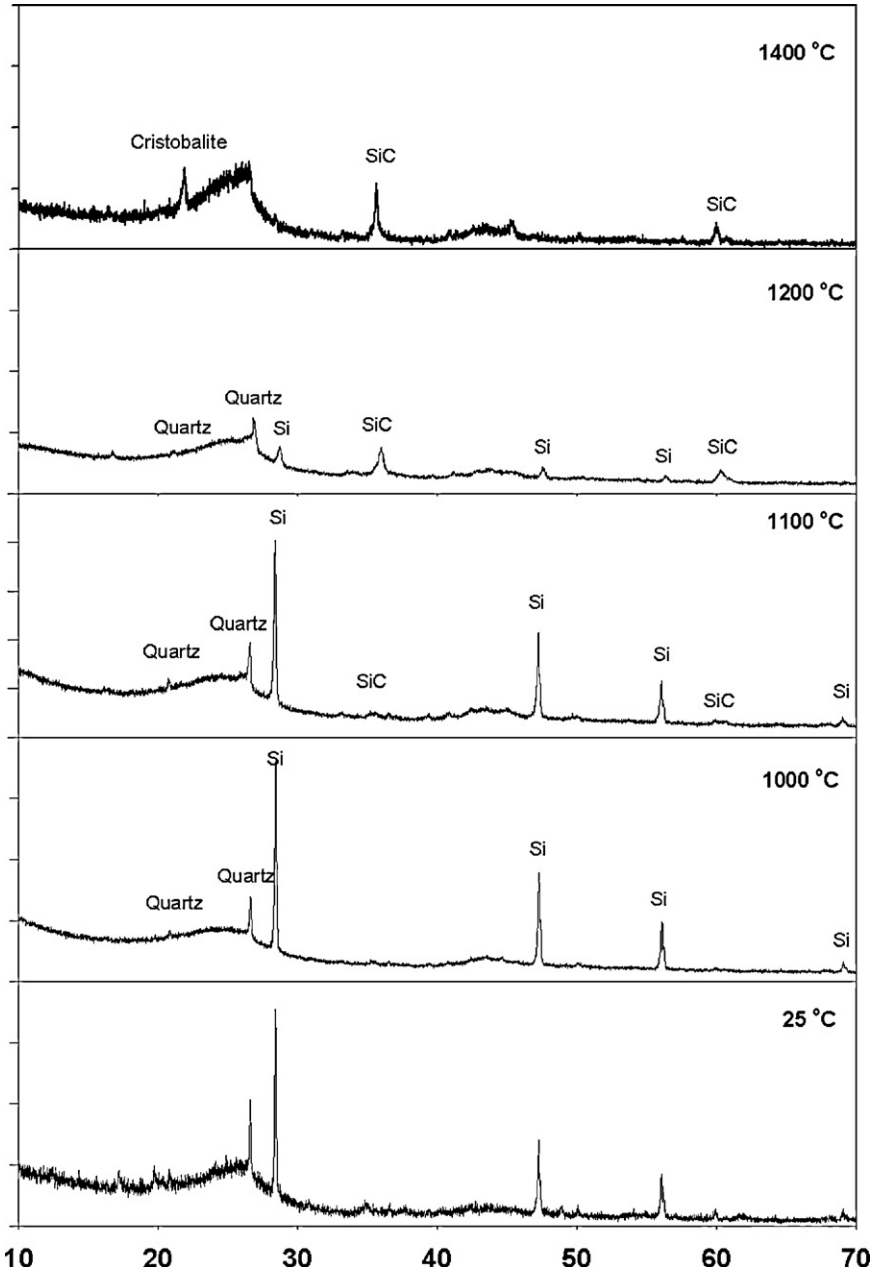

Fig. 5. Crystal structure change as temperature increased within anthracite pellets made from anthracite fines with 9% silicon content.

nanoparticles to lead the growth if VLS was the only growth mechanism.

Furthermore, the branching patterns of the SCNWs in this study can hardly be explained by VLS growth. Wang et al. indicated that the branches of nanowires obtained though VLS growth were usually epitaxial branching and were achieved through more than one step [30]. As the first step, the backbone nanowire was fully grown from a metal nanoparticle catalyst. As the next step, additional metal nanoparticles became doped on this back bone nanowires, and these facilitated branching nanowires to proceed from this backbone nanowires.

In contrast to the above multi-step mechanism, the branching nanowires in this study exhibited growth patterns that could not be readily explained by catalyst-induced epitaxial VLS growth. Indeed, Shen et al. [31] observed branching of gallium sulfide nanowires through one-step VS growth.

Another important feature for both VLS and VS growth has been the continuous supply of raw materials for the nanowire growth from the vapor phase. However, in contrast, for the study herein, the carbon and silicon instead originated from preloaded solid-phase precursors (anthracite fines and silicon powders) that were bonded together with collagen. The carbon and silicon sources should transit through a vapor phase as they participate in the vapor deposition. Conventionally, high temperature pyrolysis can volatilize some carbon from solid anthracite, yielding hydrocarbons and CO_x.

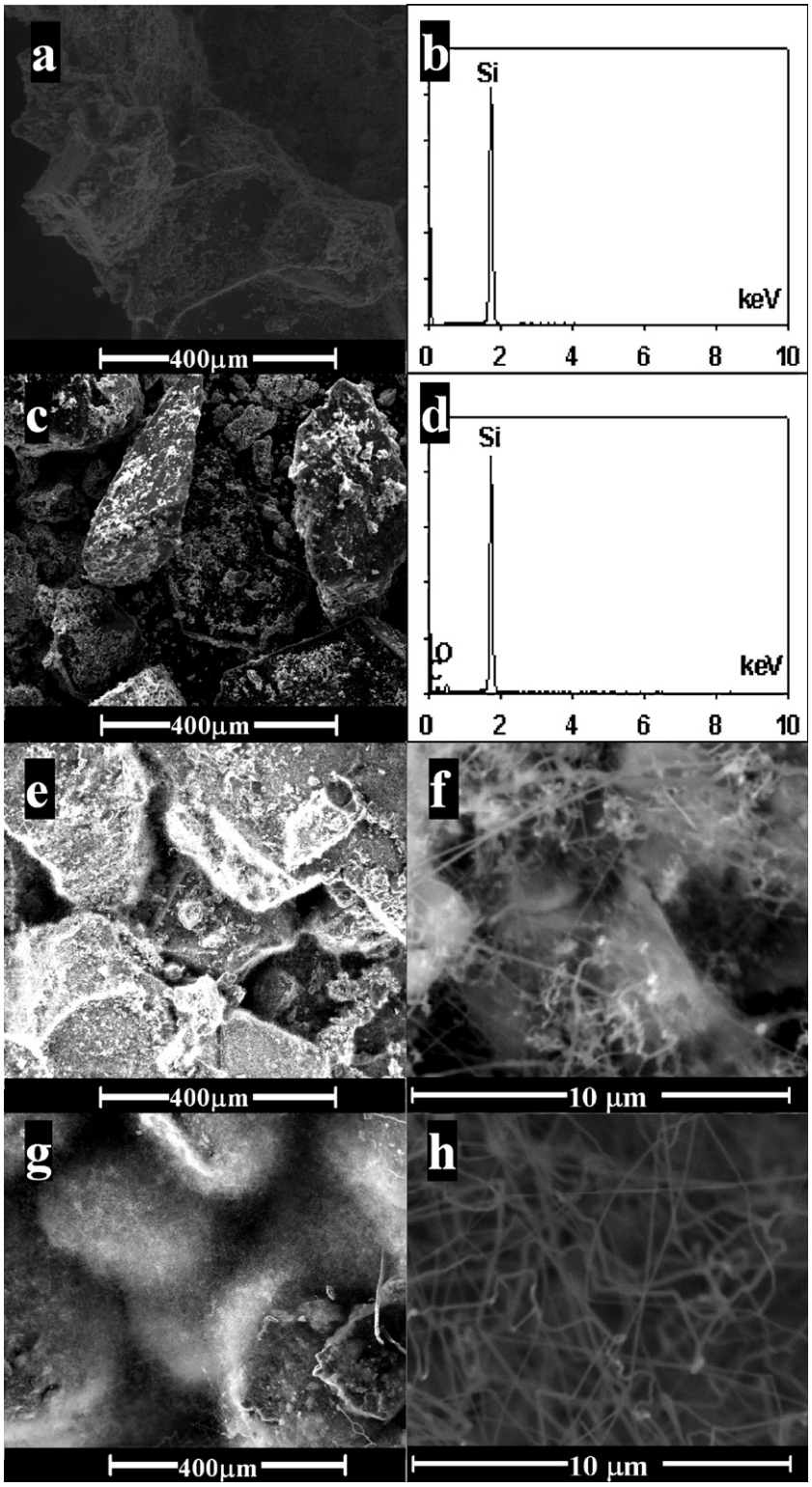

Fig. 6. Change of morphology as temperature increases within anthracite pellets made from anthracite fines with 9% silicon content (a, 25 °C; c, 1000 °C; e and,f, 1100 °C; g and h, 1200 °C; b and d show the EDS spectrums on silicon particles treated at 25 °C and 1000 °C respectively).

The fate of silicon in the presence of anthracite at high temperatures also was an important factor for the work herein. Although the melting point for silicon is higher than the pyrolysis temperatures used in this study, the silicon powders used herein apparently transformed to vapors at temperature as low as 1100 °C. It was noticed that after being pyrolyzed at 1100 °C and 1200 °C, some parts on the exterior surface of the pellets were covered by visible cotton-like fibers. These amorphous fibers contained mainly silicon and oxygen, but no carbon, as detected by EDS. They were several microns in

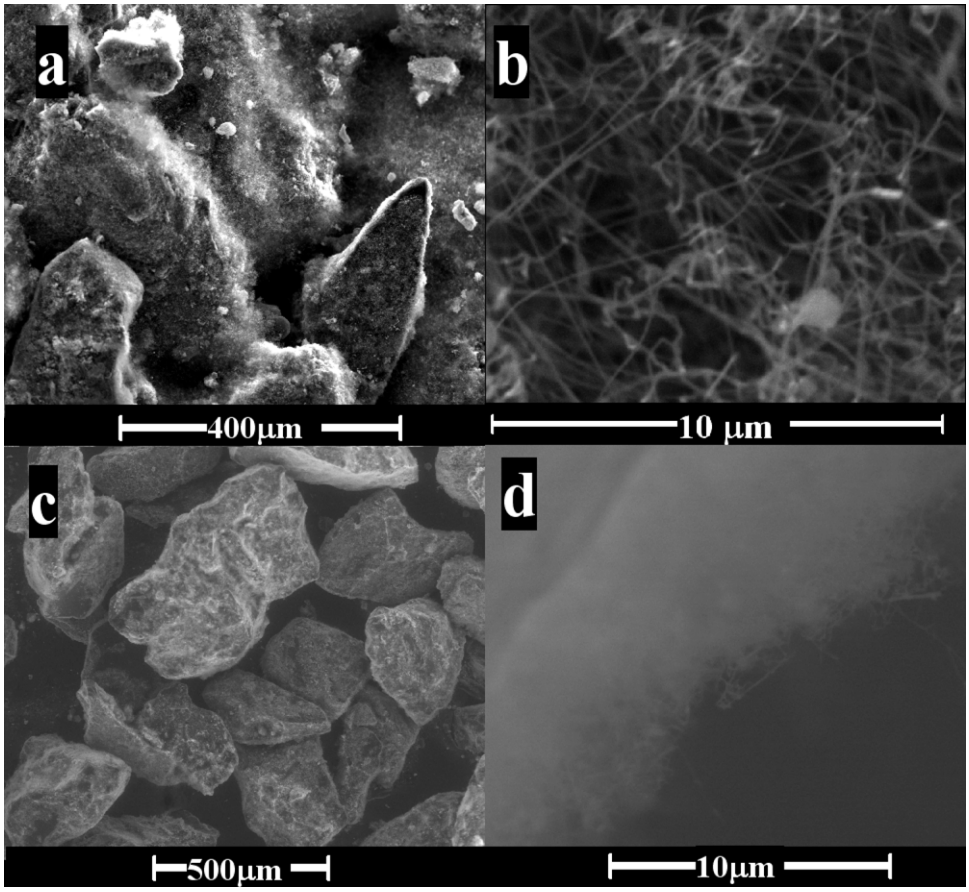

Fig. 7. SEM images of SCNWs grown from anthracite fines with different silicon contents (a and,b, 4.72%; c and,d, 1.74%) at 1400 °C.

diameter and could grow to the length of one centimeter. But these were not seen in the 1000 °C and 1400 °C products. The slower SiC forming rate at 1100 °C and 1200 °C allowed the unused silicon oxide vapor to diffuse out of the pellets and nucleate on their exterior surfaces to form the SiO_x fibers. In the case of insufficient silicon content or lower pyrolysis temperature, there was not enough supply of vaporized silicon species. This resulted in the poor growth of SCNWs with either low silicon content or at temperatures below 1100 °C.

4. Conclusion

SCNWs could be grown from anthracite surfaces through a simple protocol that employed relatively inexpensive solid precursors. The SCNWs growth could be most readily explained by a vapor–solid mechanism that exhibited no evidence of metal catalysts. The growth of SCNWs started at around 1100 °C, which was necessary to transfer Si-precursors into the vapor phase. The SCNWs produced in this study have the typical cubic zinc-blende crystal structure. Enough preloaded Si-precursor was also necessary to form the SCNWs. These nanowires provided strong binding strength that offered the very favorable performance of holding the anthracite fines together even after exposure to extremely high temperature. Results in this study showed a promising mechanism of employing SCNW formation as a means of reinforcing carbon based materials.

Acknowledgements

The authors would like to thank Dr. Hiroaki Katsuki, Saga Ceramics Lab, Japan, and Dr. Joe Kulik, at the Materials Research Institute of The Pennsylvania State University for their help with TEM analyses. The work herein was funded in part by the National Science Foundation (CMMI 0927967), Department of Energy (CPCPC), and the Ben Franklin Technology Partnerships of Pennsylvania.

References

[1] K. Takahashi, M. Yokouchi, S.K. Lee, K. Ando, Crack-healing behavior of Al_2O_3 toughened by SiC whiskers, J. Am. Ceram. Soc. 86 (December (12)) (2003) 2143–2147.
[2] X.H. Zhang, L. Xu, W.B. Han, L. Weng, J.C. Han, S.Y. Du, Microstructure and properties of silicon carbide whisker reinforced zirconium diboride ultra-high temperature ceramics, Solid State Sci. 11 (January (1)) (2009) 156–161.
[3] W. Yang, H. Araki, Q.L. Hu, N. Ishikawa, H. Suzuki, T. Noda, In situ growth of SiC nanowires on RS-SiC substrate(s), J. Cryst. Growth 264 (1–3) (2004) 278–283.
[4] W. Yang, H. Araki, S. Thaveethavorn, H. Suzuki, T. Noda, In situ synthesis and characterization of pure SiC nanowires on silicon wafer, Appl. Surf. Sci. 241 (1–2) (2005) 236–240.

[5] S.Z. Deng, Z.B. Li, W.L. Wang, N.S. Xu, J. Zhou, X.G. Zheng, et al., Field emission study of SiC nanowires/nanorods directly grown on SiC ceramic substrate, Appl. Phys. Lett. 89 (2) (2006).
[6] Y.H. Gao, Y. Bando, K. Kurashima, T. Sato, SiC nanorods prepared from SiO and activated carbon, J. Mater. Sci. 37 (10) (2002) 2023–2029.
[7] E. Munoz, A.B. Dalton, S. Collins, A.A. Zakhidov, R.H. Baughman, W.L. Zhou, et al., Synthesis of SiC nanorods from sheets of single-walled carbon nanotubes, Chem. Phys. Lett. 359 (5–6) (2002) 397–402.
[8] E.W. Wong, P.E. Sheehan, C.M. Lieber, Nanobeam mechanics: elasticity, strength, and toughness of nanorods and nanotubes, Science 277 (5334) (1997) 1971–1975.
[9] T.Y. Zhang, M. Luo, W.K. Chan, Size-dependent surface stress, surface stiffness, and Young's modulus of hexagonal prism [1 1 1] beta-SiC nanowires, J. Appl. Phys. 103 (10) (2008).
[10] X.T. Zhou, N. Wang, H.L. Lai, H.Y. Peng, I. Bello, N.B. Wong, et al., Beta-SiC nanorods synthesized by hot filament chemical vapor deposition, Appl. Phys. Lett. 74 (26) (1999) 3942–3944.
[11] D.J. Fu, X.R. Zeng, J.Z. Zou, L. Li, X.H. Li, F. Deng, In situ synthesis and photoluminescence of SiC nanowires by microwave-assisted pyrolysis of methane, J. Alloys Compd. 486 (1–2) (2009) 406–409.
[12] W. Khongwong, M. Imai, K. Yoshida, T. Yano, Synthesis of beta-SiC/SiO_2 core–shell nanowires by simple thermal evaporation, J. Ceram. Soc. Jpn. 117 (1362) (2009) 194–197.
[13] G.Y. Li, X.D. Li, H. Wang, X. Xing, Y. Yang, SiC nanowires grown on activated carbon in a polymer pyrolysis route, Mater. Sci. Eng. B: Adv. Funct. Solid-State Mater. 166 (1) (2010) 108–112.
[14] W.S. Shi, Y.F. Zheng, H.Y. Peng, N. Wang, C.S. Lee, S.T. Lee, Laser ablation synthesis and optical characterization of silicon carbide nanowires, J. Am. Ceram. Soc. 83 (12) (2000) 3228–3230.
[15] J. Zhang, Q.S. Wang, F. Wang, X.H. Chen, W.W. Lei, Q.L. Cui, et al., Plasma-assisted self-catalytic vapour–liquid–solid growth of beta-SiC nanowires, J. Phys. D: Appl. Phys. 42 (3) (2009).
[16] G. McMahon, G.J.C. Carpenter, T.F. Malis, On the growth-mechanism of silicon-carbide whiskers, J. Mater. Sci. 26 (20) (1991) 5655–5663.
[17] R.S. Wagner, W.C. Ellis, Vapor–liquid–solid mechanism of single crystal growth (new method growth catalysis from impurity whisker epitaxial + - large crystals Si E), Appl. Phys. Lett. 4 (5) (1964) 89.
[18] G.Z. Yang, H. Cui, Y. Sun, L. Gong, J. Chen, D. Jiang, et al., Simple catalyst-free method to the synthesis of beta-SiC nanowires and their field emission properties, J. Phys. Chem. C 113 (36) (2009) 15969–15973.
[19] H. Huang, Y.J. Wang, F.S. Cannon, Pore structure development of in-situ pyrolyzed coals for pollution prevention in iron foundries, Fuel Process. Technol. 90 (9) (2009) 1183–1191.
[20] G. Attolini, F. Rossi, F. Fabbri, M. Bosi, B.E. Watts, G. Salviati, A new growth method for the synthesis of 3C-SiC nanowires, Mater. Lett. 63 (29) (2009) 2581–2583.
[21] H.J. Dai, E.W. Wong, Y.Z. Lu, S.S. Fan, C.M. Lieber, Synthesis and characterization of carbide nanorods, Nature 375 (6534) (1995) 769–772.
[22] B.T. Park, Y.W. Ryu, K.J. Yong, Growth and characterization of silicon carbide nanowires, Surf. Rev. Lett. 11 (4–5) (2004) 373–378.
[23] H.J. Choi, H.K. Seong, J.C. Lee, Y.M. Sung, Growth and modulation of silicon carbide nanowires, J. Cryst. Growth 269 (2–4) (2004) 472–478.
[24] D.H. Wang, D.Q. Wang, Y.J. Hao, G.Q. Jin, X.Y. Guo, K.N. Tu, Periodically twinned SiC nanowires, Nanotechnology 19 (21) (2008).
[25] H. Katsuki, S. Furuta, S. Komarneni, Formation of novel ZSM-5/porous mullite composite from sintered kaolin honeycomb by hydrothermal reaction, J. Am. Ceram. Soc. 83 (May (5)) (2000) 1093–1097.
[26] J.S. Lee, Y.K. Byeun, S.H. Lee, S.C. Choi, In situ growth of SiC nanowires by carbothermal reduction using a mixture of low-purity SiO_2 and carbon, J. Alloys Compd. 456 (1–2) (2008) 257–263.
[27] G.Y. Li, X.D. Li, H. Wang, L. Liu, Long SiC nanowires synthesized from off-gases of the polycarbosilane-derived SiC preparation, Appl. Phys. A: Mater. Sci. Process. 98 (2) (2010) 293–298.
[28] Y.J. Zhang, N.L. Wang, R.R. He, X.H. Chen, J. Zhu, Synthesis of SiC nanorods using floating catalyst, Solid State Commun. 118 (11) (2001) 595–598.
[29] S.Z. Deng, Z.S. Wu, J. Zhou, N.S. Xu, R. Chen, J. Chen, Synthesis of silicon carbide nanowires in a catalyst-assisted process, Chem. Phys. Lett. 356 (5–6) (2002) 511–514.
[30] D. Wang, F. Qian, C. Yang, Z.H. Zhong, C.M. Lieber, Rational growth of branched and hyperbranched nanowire structures, Nano Lett. 4 (May (5)) (2004) 871–874.
[31] G.Z. Shen, D. Chen, P.C. Chen, C.W. Zhou, Vapor–solid growth of one-dimensional layer-structured gallium sulfide nanostructures, ACS Nano 3 (5) (2009) 1115–1120.